https://doi.org/10.5194/acp-2020-364
Preprint. Discussion started: 14 May 2020

Atmospheric Chemistry and Physics Discussions

Increased new particle yields with largely decreased probability of survival to CCN size at the summit of Mt. Tai under reduced SO_2 emissions

Yujiao Zhu[1], Likun Xue[1,2*], Jian Gao[3], Jianmin Chen[4], Hongyong Li[1], Yong Zhao[5], Zhaoxin Guo[5], Tianshu Chen[1], Liang Wen[1], Penggang Zheng[1], Ye Shan[1], Xinfeng Wang[1], Tao Wang[6], Xiaohong Yao[7*], Wenxing Wang[1]

[1]Environment Research Institute, Shandong University, Qingdao 266237, China

[2]Collaborative innovation Center for climate Change, Jiangsu Province, Nanjing, 210023, China

[3]Chinese Research Academy of Environmental Sciences, Beijing 100012, China

[4]Shanghai Key Laboratory of Atmospheric Particle Pollution and Prevention (LAP3), Department of Environmental Science & Engineering, Fudan University, Shanghai 200433, China

[5]Taishan National Reference Climatological Station, Tai'an 271000, China

[6]Department of Civil and Environmental Engineering, Hong Kong Polytechnic University, Hong Kong, China

[7]Key Lab of Marine Environmental Science and Ecology, Ministry of Education, Ocean University of China, Qingdao 266100, China

Correspondence to: Likun Xue (xuelikun@sdu.edu.cn) and Xiaohong Yao (xhyao@ouc.edu.cn)

Abstract. Because anthropogenic sulfur dioxide (SO_2) emissions have decreased considerably in the last decade, $PM_{2.5}$ pollution in China has been alleviated to some extent. However, the effects of reduced SO_2 on the particle number concentrations and subsequent contributions of grown new particles to the cloud condensation nuclei (CCN) populations, particularly at high altitude with low aerosol number loadings, are poorly understood. In this study, we evaluated the campaign-based measurements made at the summit of Mt. Tai (1534 m a.s.l.) from 2007 to 2018. With the decrease in the SO_2 mixing ratios from 15 ± 13 ppb in 2007 to 1.6 ± 1.6 ppb in 2018, the formation rate of new particles (FR) and the net maximum increase in the nucleation-mode particle number concentration (NMINP) increased by 2–3 fold in 2018 against those in 2007. In contrast, the occurrence frequency of new particle formation (NPF) events in which the maximum geometric median diameter of grown new particles (D_{pgmax}) was >50 nm decreased considerably from 43%–78% of the NPF events before 2015 to <12% in 2017–2018. Assuming >50 nm as a CCN threshold size at high supersaturations, the observed net CCN production decreased from 3703 cm^{-3} (on average) before 2015 to 1026 cm^{-3} (on average) in 2017–2018. We argue that the increase in the FR and NMINP is mainly determined by the availability of organic precursors that participate in nucleation and initial growth, whereas the decrease in the growth probability is caused by the reduced emissions of anthropogenic precursors. However, large uncertainties still exist because of a lack of data on the chemical composition of these smaller particles.

https://doi.org/10.5194/acp-2020-364
Preprint. Discussion started: 14 May 2020


Atmospheric Chemistry and Physics Discussions

1. Introduction

Atmospheric new particle formation (NPF) is regarded as an important source of aerosol particles in terms of number concentrations, and the newly formed particles can grow into a variety of sizes with different functions. For example, particles larger than 50–80 nm may act as cloud condensation nuclei (CCN), whereas those larger than 100 nm may directly affect solar radiation (Kulmala and Kerminen, 2008; Kerminen et al., 2012; Seinfeld and Pandis, 2012). Sulfuric acid (H_2SO_4) is considered as the key nucleating precursor for NPF, and other species, such as ammonia (NH_3), amines, and highly oxygenated molecules [HOMs—oxidation products of volatile organic compounds (VOCs)] can also participate and enhance nucleation in the continental troposphere (Ehn et al., 2014; Tröstl et al., 2016; Yao et al., 2018; Kerminen et al, 2018; Chu et al., 2019; Lee et al., 2019). The subsequent growth of new particles is affected by not only the abovementioned precursors but also the semi-volatile compounds (Riipinen et al., 2012; Ehn et al., 2014; Tröstl et al., 2016).

NPF events have been reported widely throughout the world, including in the severely polluted urban and rural areas in China that experience high sulfur dioxide (SO_2) concentrations and high aerosol loading (Kulmala et al., 2004; Gao et al., 2009; Guo et al., 2012; Nie et al., 2014; Kerminen et al., 2018; Chu et al., 2019). In the last few decades, anthropogenic emissions of gaseous and particulate air pollutants in China have been reduced substantially due to the rigorous emission control policies. Between 2007 and 2018 (the observation period in this study), the national total SO_2 emissions decreased by 67% (from 24.7 million tons to 8.2 million tons), and the national average ambient SO_2 concentrations decreased by 73% (from 17.9 ppb to 4.9 ppb, see Fig. S1). The North China Plain (NCP) region experiences the most severe SO_2 pollution, which has shown a visible decreasing trend since 2011 (Krotkov et al., 2016; Fan et al., 2020). Such huge reductions in SO_2 emissions may alter the frequency and intensity of NPF events and the subsequent growth of new particles. The changes in the mixing ratios of VOC components, ambient oxidants, aerosol loading, and meteorological factors may also influence the NPF events, yielding more complex and uncertain feedbacks (Kulmala and Kerminen, 2008; Zhang et al., 2012).

The long-term changes in the NPF events under reduced SO_2 conditions have been studied in several cities in Europe and the U.S. For example, decreased NPF frequency and reduced new particle yields accompanied by a decline in the SO_2 concentrations were observed in Pittsburgh (U.S.), Rochester (U.S.), and Melpitz (Germany) (Hamed et al., 2010; Wang et al., 2011, 2017; Saha et al., 2018). In contrast, long-term studies in Pallas (Finland), Hyytiälä (Finland), and Crete (Greece) showed no trend in the NPF frequency despite a considerable decrease in the ambient SO_2 concentrations all over Europe (Asmi et al., 2011; Nieminen et al., 2014; Kalivitis, et al., 2019). Moreover, a slightly upward trend in the particle formation and growth rates was observed in Pallas and Hyytiälä, attributable to the increased biogenic VOC (BVOC) emissions (Asmi et al., 2011; Nieminen et al., 2014). In China, the earliest observation of NPF events started around 2004 in Beijing (Wu et al., 2007). Comparison of tens of independent experiments showed that the NPF frequency has remained relatively constant until recent years, probably due to the reduced production and reduced loss rate of H_2SO_4, which may have canceled each other out to some extent in Beijing (Chu et al., 2019; Li et al., 2020). However, the long-term changes in NPF intensities and

https://doi.org/10.5194/acp-2020-364
Preprint. Discussion started: 14 May 2020


Atmospheric Chemistry and Physics Discussions

the subsequent growth of new particles have not been studied in China, where the anthropogenic emissions of various air pollutants have been changing significantly in the past decade.

In this study, we analyzed the measurement data of particle number concentrations, chemical compositions, trace gases, and meteorological parameters collected at the summit of Mt. Tai (36.25°N, 117.1°E, 1534 m a.s.l.) during seven observational campaigns from 2007 to 2018. Mt. Tai is the highest mountain in the NCP, located at the region's center, and the observation station has been widely deployed to investigate the regional air pollution as well as transport and chemical processes in the NCP (Gao et al., 2005; Li et al., 2011; Sun et al., 2016; Wen et al., 2018). Moreover, the summit is close to the top of the planetary boundary layer or even in the free troposphere sometimes, and is characterized by fewer pre-existing particles, stronger UV solar radiation, and lower ambient temperature, which favor NPF events (Li et al., 2011; Shen et al., 2016a; Lv et al., 2018;). The contribution of new particles, compared with that of primary particles, to CCN population reportedly increases at higher elevations, indicating a critical role of high-altitude NPF in cloud formation and related climate impacts (Merikanto et al., 2009). Our study aimed to examine the effects of reduced SO_2 emissions on the regional NPF events in terms of their occurrence frequency, and intensity and the subsequent growth of new particles at high altitudes.

2. Methods

2.1 Experimental

This study comprised seven intensive campaigns from 2007 to 2018, and the details are summarized in Table 1. The duration of each campaign varied from 18 days to 71 days. The measurement data obtained in the four campaigns in 2007, 2014, and 2015 have been reported by Gao et al. (2008) and Lv et al. (2018), and here, all of the available data were combined to derive the decadal trends in NPF events.

All measurements were obtained using commercial instruments, which have been described in previous studies (e.g., Zhou et al., 2009; Zhu et al., 2017; Lv et al., 2018). During the seven campaigns, particle number size distributions (PNSDs) were monitored using a wide-range particle spectrometer (*WPS; Model 1000XP, MSP Corporation, USA*) at ambient relative humidity (RH) conditions. The WPS combines a differential mobility analyzer (DMA), a condensation particle counter (CPC), and a laser particle spectrometer (LPS). The DMA and CPC can measure particles in the 5–500 nm (or 10–500 nm) size range and were set up to 48 channels. The LPS covers the size range of 350 nm–10 μm and was divided into 24 channels. Occasionally, the data quality was poor at the bins around 330 nm; therefore, we used 10–300 nm particles for calculations in all campaigns except for that in spring of 2007, when the data of >153 nm particles were missing and we used data of 10–150 nm particles instead for calculation.

Trace gases were monitored during each campaign. SO_2 was measured using an ultraviolet fluorescence analyzer (*Model 43C, Thermo Electron Corporation, USA*); O_3 was monitored using two ultraviolet absorption analyzers (*Model 49C, Thermo Electron Corporation, USA*, or *Model 400U, Advanced Pollution Instrumentation Inc., USA*); NO and NO_2 were

https://doi.org/10.5194/acp-2020-364
Preprint. Discussion started: 14 May 2020


Atmospheric Chemistry and Physics Discussions

monitored using a chemiluminescence analyzer (*Model 42C or 42i, Thermo Electron Corporation, USA*) equipped with a blue light converter before August 2014 and subsequently using a chemiluminescence analyzer (*Model T200U, API, USA*) and a cavity-attenuated phase-shift spectroscopy instrument (*Model T500U, API, USA*), respectively. The inorganic water-soluble ions in $PM_{2.5}$ together with acid and alkaline gases were measured using an online Ambient Ion Monitor (*URG-AIM 9000B, URG Corporation, USA*; only for water-soluble ions in $PM_{2.5}$) in 2007 and using a Monitor for Aerosols and Gases (*MARGA; ADI20801, Applikon-ECN, Netherlands*) in the five campaigns from 2014 onward. Data of the meteorological parameters including temperature (T), RH, wind speed, wind directions, and precipitation were provided by the Mt. Tai Meteorological Station.

Air mass back trajectories were calculated using the Hybrid Single Particle Lagrangian Integrated Trajectory (HYSPLIT) model. The input meteorological data [Global Data Analysis System (GDAS) data] were used with 1° latitude–longitude resolution. The trajectory ending height of 1400 m a.g.l. was selected because the terrain height on Mt. Tai was approximately 150 m in the GDAS data.

2.2 Calculation methods

2.2.1 Definition of NPF events and relevant parameters

In this study, particles with diameter smaller than 25 nm were defined as nucleation mode particles (Kulmala et al., 2012). NPF events can be identified as distinct bursts of new nucleation mode particles, which keep growing larger over a period of time (Dal Maso et al., 2005; Hirsikko et al., 2007; Kulmala et al., 2012). The end time of an NPF event was defined as the time when the particle number concentrations approached the background levels observed before the NPF event. The NPF event duration was defined as the time duration between the start time and end time of an NPF event.

Three parameters are commonly used to evaluate the NPF characteristics, viz., new particle formation rate (FR), growth rate (GR), and condensation sink (CS) (Sihto et al., 2006; Kulmala et al., 2012), and were calculated here following the method described by Zhu et al. (2017 and 2019; and see supplementary materials). The net maximum increase in the nucleation-mode particle number concentration (NMINP) was also calculated as described by Zhu et al. (2017 and 2019).

$$\mathrm{NMINP} = N_{10\text{–}25\ \mathrm{nm}}(t_1) - N_{10\text{–}25\ \mathrm{nm}}(t_0) \quad (1)$$

where $N_{10\text{–}25\ \mathrm{nm}}$ is the sum of nucleation mode particle number concentrations, and t_0 and t_1 represent the time of an NPF event to be initially observed and the time when $N_{10\text{–}25\ \mathrm{nm}}$ reaches the maximum value, respectively.

D_{pg} represents the geometric median diameter of new particles and was fitted by a multi log-normal distribution function (Whitby, 1978; Zhu et al., 2014, 2019; Man et al., 2015). Varying size ceilings occurred during the growth of newly formed particles, and the maximum size of D_{pg} was defined as D_{pgmax} (Zhu et al., 2019).

https://doi.org/10.5194/acp-2020-364
Preprint. Discussion started: 14 May 2020


Atmospheric Chemistry and Physics Discussions

As shown in Fig. 1, the NPF events were classified into three categories according to the different sizes of D_{pgmax}. In Category 1 events (e.g., December 25, 2017, Fig. 1a), the new particles grow to D_{pgmax} of <50 nm, which is too small to serve as CCN. In Category 2 events (e.g., April 7, 2018, Fig. 1b), the new particles grow to D_{pgmax} of 50–80 nm. In Category 3 events (e.g., December 24, 2017, Fig. 1a), the new particles grow to D_{pgmax} of >80 nm. The NPF events in Categories 2 and 3 can be regarded as climate-relevant events.

2.2.2 Sulfuric acid proxy

The proxy for H_2SO_4 concentration could be roughly estimated based on the solar radiation (SR), SO_2 concentration, CS, and RH as follows (Mikkonen et al., 2011; Lv et al., 2018):

$$[H_2SO_4] = 8.21 \times 10^{-3} \cdot k \cdot SR \cdot [SO_2]^{0.62} \cdot (CS \cdot RH)^{-0.13} \quad (2)$$

where k is a temperature-dependent reaction rate constant, and SR was estimated from the HYSPLIT model.

The contribution of H_2SO_4 vapor to the particle growth from D_{p0} to D_{p1} can be expressed by the following equation (Kulmala et al., 2001):

$$R = ([H_2SO_4]_{avg}/C) \times 100\% \quad (3)$$

where $[H_2SO_4]_{avg}$ is the average concentration of H_2SO_4 during the particle growth period, and C is the total concentration of condensable vapor for the particle growth from D_{p0} to D_{p1}, which can be calculated as described by Kulmala et al. (2001). Notably, uncertainty may exist in the estimated contribution of the SO_2 concentrations and radiation intensity to H_2SO_4, as well as in the contribution of H_2SO_4 to the particle growth.

2.2.3 CCN parameters

In the absence of direct CCN measurements, the potential contribution of new particles to the CCN population can be estimated from the particle number size distribution (Lihavainen et al., 2003; Rose et al., 2017). Theoretically, particles larger than 50 nm (i.e., 80 nm) can be activated as CCN under quite high (moderate) supersaturation (Dusek et al., 2006; Petters and Kreidenweis, 2007; Ma et al., 2016), and particles larger than 100 nm can directly impact climate by scattering and absorbing solar radiation (Charlson et al., 1992; Seinfeld and Pandis, 2012). In this study, we introduced three terms: the net increase of NPF-derived CCN number concentration (ΔN_{CCN}), the survival probability of new particles to CCN sizes (SP), and the relative increase ratio of CCN population (R_{CCN}). Three sizes, viz., 50 nm, 80 nm, and 100 nm, were defined as the CCN threshold sizes. ΔN_{CCN} was calculated following the method of Rose et al. (2017):

$$\Delta N_{CCN} = N_{CCN}(t'_1) - N_{CCN}(t_0) \quad (4)$$

where the N_{CCN} terms represent the potential CCN number concentrations and were estimated from the number concentrations of particles larger than 50 nm, 80 nm, and 100 nm (N_{CCN50}, N_{CCN80}, and N_{CCN100}, respectively); t_0 is the time

https://doi.org/10.5194/acp-2020-364
Preprint. Discussion started: 14 May 2020


Atmospheric Chemistry and Physics Discussions

when an NPF event is initially observed, same to that in equation (1); and t'_1 is the time when the N_{CCN} reaches the maximum value during the new particle growth periods. Each concentration was taken as 1-h average. The ΔN_{CCN} eliminates the influence of pre-existing particles.

The SP was calculated as described by Zhu et al. (2019):

$$SP = \Delta N_{CCN}/NMINP \quad (5)$$

R_{CCN} values were the ratios of NPF-derived CCN to pre-existing CCN and were calculated as follows:

$$R_{CCN} = \Delta N_{CCN}/N_{CCN}(t_0) \quad (6)$$

3. Results

3.1 Variation in the NPF frequency

During the seven campaigns, NPF events were observed on 106 of the 265 sampling days. As shown in Fig. 2, the NPF frequencies in three seasons of different years were surprisingly almost the same, i.e., 50% in the spring of 2007, 50% in the summer of 2009, 49% in the winter of 2017, and 51% in the spring of 2018. However, the NPF frequency decreased to 42% in the summer of 2014, 33% in the fall of 2014, and 20% in the summer of 2015. The low NPF frequencies were likely caused by the unfavorable weather conditions. For example, there were 15 rainy days out of the 40 sampling days during the 2015 summer campaign, but only 3 rainy days out of the total 18 sampling days in the 2009 summer campaign.

When Categories 1, 2, and 3 of NPF events were examined separately, the Category 1 NPF frequencies in the winter of 2017 (43%) and the spring of 2018 (49%) were significantly higher than those before (5%–21%; $p < 0.05$). Category 2 events were absent in the winter of 2017, whereas Category 3 events were absent in the spring of 2018. The sums of Category 2 and 3 NPF frequencies were significantly lower in 2017 (6%) and 2018 (3%) than before (14%–39%; $p < 0.05$), even in comparison with the lower NPF frequencies in the summer of 2015 (15%) and the fall of 2014 (14%). When the sums of Category 2 and 3 NPF frequencies in each campaign were normalized by the corresponding total NPF frequency, the boundary was clearer, i.e., the normalized sum values were as high as 43%–78% before 2015 and <12% in 2017–2018. Clearly, the newly formed particles observed at Mt. Tai had been less climatically relevant in 2017–2018 compared with those before 2015, despite the comparable NPF frequencies.

3.2 Variations in the FR, NMINP, GR, and D_{pgmax}

We used four metrics, i.e., the FR, NMINP, GR, and D_{pgmax}, to characterize the NPF events and evaluate potential climate impacts of the grown new particles (Fig. 3). During the four campaigns in 2007, 2009, and 2014, the calculated FR varied narrowly in each campaign and the campaign average narrowed to 0.8–1.2 cm^{-3} s^{-1}. The FR increased thereafter, i.e., 2.6 ± 1.3 cm^{-3} s^{-1} in 2015, 2.0 ± 1.7 cm^{-3} s^{-1} in 2017, and 3.0 ± 2.7 cm^{-3} s^{-1} in 2018. The FRs were 3–7 times lower than

https://doi.org/10.5194/acp-2020-364
Preprint. Discussion started: 14 May 2020


Atmospheric Chemistry and Physics Discussions

those obtained from the measurements down to 3 nm simultaneously made by twin differential mobility particle sizer (TDMPS) or neutral cluster and air ion spectrometer (NAIS) at the same site during previous campaigns (Shen et al., 2016a,b; Lv et al., 2018).

The NMINP showed a temporal variation trend similar to that shown by the FR (Fig. 3b). The campaign average NMINP varied in a narrow range of 3.8–5.1 × 10^3 cm^{-3} in 2007–2014, but then showed an increasing trend from 6.3 ± 2.6 × 10^3 cm^{-3} in 2015, 9.4 ± 7.9 × 10^3 cm^{-3} in 2017, to 1.1 ± 1.0 × 10^4 cm^{-3} in 2018. The increase in the NMINP should enhance the contribution of NPF events to the ambient particle number concentration, but the NMINP at Mt. Tai before 2015 was only approximately ¼–½ of our previous observations in urban and marine atmospheres (Zhu et al., 2017, 2019).

Unlike the increasing trends in the FR and NMINP from 2007 to 2018, the GR showed a strongly season-dependent trend (Fig. 3c). Higher GRs were generally observed in the summer campaigns, with the three campaign averages in the range of 7.3–9.6 nm h^{-1}, consistent with those reported in the literature, because of enhanced photochemical reactions and biological activities (Kulmala et al., 2004; Chu et al., 2019). The reverse was true in winter, and a lower GR was expectedly observed in the winter of 2017, i.e., 2.3 ± 1.3 nm h^{-1}. The GRs in the spring and fall campaigns ranked between those of summer and winter campaigns. The average GR in the spring of 2007 (4.4 ± 2.3 nm h^{-1}) was slightly higher than that in the spring of 2018 (3.3 ± 2.3 nm h^{-1}), although the FR and NMINP increased considerably in the latter spring campaign. The average GR was 4.9 ± 2.7 nm h^{-1} in the fall of 2014.

The D_{pgmax} is partially determined by the GR. The largest campaign average D_{pgmax} of 84 ± 39 nm expectedly appeared in the summer of 2009, followed by 71 ± 24 nm in the summer of 2015. However, the campaign average D_{pgmax} was only 60 ± 18 nm in the summer of 2014, followed by 59 ± 18 nm in the spring of 2007, 53 ± 22 nm in the fall of 2014, and 48 ± 58 nm in the winter of 2017. The campaign average D_{pgmax} in the spring of 2018 was the lowest, i.e., 29 ± 13 nm, although the campaign average GR was even larger than that in the winter of 2017. These findings indicate that the D_{pgmax} is clearly determined not only by the GR but also by unidentified factors, which will be addressed in Section 4.2.

In summary, we found an increasing trend in the FR and NMINP from 2007 to 2018. The GR showed strong season dependence, without any inter-annual variations. The D_{pgmax} was significantly lower in 2018, but the GR alone cannot explain the lower values.

3.3 Potential contribution to CCN production from the NPF events

Direct measurements of the CCN were not available; therefore, potential contributions of the grown new particles to the CCN population were estimated using equations (4)–(6). The contributions varied considerably between campaigns (Fig. 4). In general, the NPF-derived CCNs were seasonally dependent, i.e., the highest number concentrations occurred in summer, followed by spring, fall, and winter. With an increase in the threshold diameters, roughly corresponding to a decrease in supersaturation from >0.6% to <0.1% (Li et al., 2015), the estimated contributions decreased because new particles were

https://doi.org/10.5194/acp-2020-364
Preprint. Discussion started: 14 May 2020


Atmospheric Chemistry and Physics Discussions

continuously removed either by coagulation or atmospheric deposition during the particle growth. During the three summer campaigns in 2009, 2014, and 2015, larger NPF-derived CCNs were estimated with average ΔN_{CCN50}, ΔN_{CCN80}, and ΔN_{CCN100} of 4.4 ± 2.5 × 10^3 cm^{-3}, 1.9 ± 1.5 × 10^3 cm^{-3}, and 1.0 ± 0.9 × 10^3 cm^{-3}, respectively. Overall, the values decreased by approximately 50% in the spring of 2007 and the fall of 2014. The NPF-derived CCNs in these five campaigns were larger than those reported in the previous studies for the same season at Mt. Chacaltaya (5240 m, Bolivia) and Botsalano (1424 m, South-Africa) (Kerminen et al., 2012; Rose et al., 2017). In comparison, extremely low NPF-derived CCNs were observed in 2017 and 2018, i.e., ΔN_{CCN50} of only 1.1 ± 1.7 × 10^3 cm^{-3}, ΔN_{CCN80} of 0.5 ± 0.9 × 10^3 cm^{-3}, and ΔN_{CCN100} of 0.2 ± 0.5 × 10^3 cm^{-3}.

High SPs were found during the three summer campaigns in 2009, 2014, and 2015, with average SP_{CCN50}, SP_{CCN80}, and SP_{CCN100} of 114%, 51%, and 28%, respectively (Fig. 4b). Notably, the SP_{CCN50} of >100% implied that almost all new particles could grow larger than 50 nm. The SPs decreased by approximately 50% in the spring of 2007 and the fall of 2014. In 2017 and 2018, the average SP_{CCN50}, SP_{CCN80}, and SP_{CCN100} were only 14%, 7%, and 3%, respectively, indicating that only a minor fraction of new particles could grow to CCN sizes before being scavenged. It appears that the lower NMINP occasionally led to higher SPs. For example, the highest SP_{CCN50}, SP_{CCN80}, and SP_{CCN100} of 149%, 64%, and 32%, respectively, were observed in the summer of 2014, and the lowest NMINP was also obtained in that campaign. Note that the spatial-temporal heterogeneity during NPF events could also result in high SPs of >100% in some cases (e.g., Fig. S2).

Figure 4c shows the percentage increase in the NPF-derived CCN relative to the pre-existing CCN. The percentages were the highest in the summer of 2014, e.g., 676%, 597%, and 482% for R_{CCN50}, R_{CCN80}, and R_{CCN100}, respectively. This finding could be attributable to the combination of high ΔN_{CCN} and low number concentrations of pre-existing particles in that campaign (Fig. S3). In the remaining four campaigns during 2007–2015, the percentages still exceeded 100%, i.e., 250%–380% for R_{CCN50}, 150%–290% for R_{CCN80}, and 110%–280% for R_{CCN100}. These ratios are within the range reported in the literature (50%–1100%), although the calculation methods were slightly different between the studies (Lee et al., 2019). However, in 2017 and 2018, the percentages decreased considerably, e.g., <40% for R_{CCN50} and <20% for R_{CCN80} and R_{CCN100}. It appears that a turn point occurred during 2017 or even earlier, but no data from 2016 were available to confirm this.

4. Discussion

4.1 Question 1: what caused the unexpected responses of NPF to reduced SO_2 concentrations?

H_2SO_4 oxidized from ambient SO_2 is one of the most important precursors for atmospheric nucleation. Decreases in ambient SO_2 mixing ratios, e.g., an annual average concentration decrease from 9 ppb to 1 ppb in Pittsburgh, 5 ppb to 3 ppb in Rochester, and 5 ppb to 2 ppb in Melpitz, have been reported to cause 40%–60% reduction in the NPF occurrence frequency and 40%–70% reduction in the NPF intensity (e.g., Hamed et al., 2010; Wang et al., 2011, 2017; Saha et al., 2018). However, this was not the case at the summit of Mt. Tai, where the NPF occurrence frequencies were almost invariant in the

https://doi.org/10.5194/acp-2020-364
Preprint. Discussion started: 14 May 2020


Atmospheric Chemistry and Physics Discussions

spring of 2007, summer of 2009, winter of 2017, and spring of 2018. The observed SO_2 mixing ratios in this study decreased considerably from 15 ± 13 ppb in 2007 to 1.6 ± 1.6 ppb in 2018 (SO_2 during NPF periods decreased from 17 ± 11 ppb to 2.8 ± 1.8 ppb, Fig. 5a). In addition, SO_2 emissions in China were reduced by approximately two-thirds from 2007 to 2018 (Fig. S1), and the sharpest reduction occurred in 2015–2016 owing to stringent mitigation policies.

As the calculated CSs before the NPF events increased in the 2017 and 2018 campaigns relative to those in the 2007 and 2009 campaigns (Fig. 5b), CSs were unlikely the cause for the non-decrease in the NPF occurrence frequency in 2017 and 2018. It has been reported that a low CS is not necessary to promote NPF occurrence at altitudes higher than 1000 m (Sellegri et al., 2019). Thus, other factors such as meteorological conditions and biogenic precursors (e.g., amines and highly oxidized organics) may overwhelm SO_2 and CS in determining the NPF occurrence frequency at Mt. Tai.

We further conducted a few statistical tests to explore the association of the FR and NMINP with SO_2. The correlation analysis using the campaign averages showed weak negative correlations of FRs and NMINPs with SO_2 mixing ratios ($r = 0.4$ and 0.3, respectively; both $p > 0.05$). Again, these results implied that other factors overwhelmed SO_2 mixing ratios in determining the FRs and NMINPs. When the observations were analyzed case by case, the correlations of the FRs and NMINPs with SO_2 mixing ratios were even weaker, with $r = -0.12$ and -0.14, respectively (both $p > 0.05$). Similar results were found when the estimated H_2SO_4 vapor was used for correlation analysis ($r = -0.12$ and -0.13, respectively; both $p > 0.05$, Fig. S4).

Table 2 provides a comprehensive comparison of the measured ambient conditions between the spring of 2007 and 2018. It shows that the decrease in SO_2, estimated H_2SO_4 concentration, and NH_3 did not explain the increases in the FRs and NMINP in 2018. Although amines were not measured, they are usually highly correlated with NH_3 (Xie et al., 2018). Based on the unique roles of HOMs in enhancing atmospheric nucleation and promoting the growth of new particles (Paasonen et al., 2010; Ehn et al., 2014; Kerminen et al., 2018), HOMs were speculated to play an important role in determining the unexpected responses of NPF to reduced SO_2 in 2018. However, we had no measurements of HOMs. Nevertheless, the correlation between the FR and NMINP at Mt. Tai appears to support the hypothesis as presented below.

During the 106 cases of NPF events, the FR and NMINP showed a good linear correlation ($r = 0.84$, $p < 0.01$) (Fig. 6). The fitted equation was highly consistent with those derived for urban and marine atmospheres (Man et al., 2015; Zhu et al., 2017, 2019; Ma et al., 2020). The strong linear relationship between the FR and NMINP suggested that H_2SO_4 vapor was sufficient for nucleation, and the NPF intensity was very likely determined by the abundance of organic vapors available for participating in nucleation. Following the equation in the literature, i.e., $FR = k_{NucOrg}[H_2SO_4]^m [NucOrg]^n$ (k_{NucOrg} as a constant, and m and n as integers; Zhang et al., 2012), the FR is controlled by the concentrations of both H_2SO_4 vapor and organic vapor. We then considered two technical terms, i.e., the total concentration of H_2SO_4 vapor and the consumed amount of H_2SO_4 vapor for NPF. Unlike the FR, the NMINP was always determined by the consumed amount of H_2SO_4 vapor, which may or may not have a positive correlation with the total concentration of H_2SO_4 vapor. The linear correlation

https://doi.org/10.5194/acp-2020-364
Preprint. Discussion started: 14 May 2020


Atmospheric Chemistry and Physics Discussions

between the FR and NMIMP suggests one possibility, i.e., the H_2SO_4 vapor was sufficient and the availability of organic vapor determined both the FR and the consumed amount of H_2SO_4 vapor proportional to the NMINP. Previous field measurements have shown that gaseous H_2SO_4 in concentrations of 10^5 molecules/cm^3 is necessary for NPF (McMurry et al., 2005; Nieminen et al., 2009; Erupe et al., 2010; Lee et al., 2019). In this study, the estimated H_2SO_4 concentration was in the range of 10^6–10^7 molecules/cm^3 and theoretically sufficient for NPF (Table 2). Under other conditions, poor correlations are expected between the FR and NMIMP, e.g., with FR > 8 cm^{-3} s^{-1} reported in previous studies (gray cross markers in Fig. 6).

Previous studies have reported that the BVOC emissions over the NCP have substantially increased in the last decade because of changes in land use and climate (Stavrakou et al., 2014; Ma et al., 2019). During our observations, the TVOC mixing ratios approached 16.1 ± 6.5 ppb in the 2018 spring campaign, which was almost double that in the June 2006 campaign (Mao et al., 2009; no data from the spring 2007 campaign were available). However, the increase in TVOC and BVOC emissions in 2018 cannot provide sufficient direct information about the increase in nucleating organics, and the measurements of H_2SO_4 at Mt. Tai were unavailable. Thus, the unexpected response of NPF events to reduced SO_2 remains a puzzle, and more measurements of organics (e.g., HOMs) are needed. Note that the campaign average of $PM_{2.5}$ mass concentration in 2018 indeed decreased. The decrease was apparently determined by the decrease in particles larger than 300 nm. Thus, the CS still increased in 2018 compared with that in 2007.

4.2 Question 2: Did the contribution of NPF events to CCN population decrease considerably with SO_2 reduction?

Based on the observations alone, the D_{pgmax} and the contribution of NPF to CCN population decreased considerably with the reduction in SO_2. However, uncertainties still exist, e.g., 1) the data size was small, and we should be cautious in extending the conclusion to a large spatiotemporal scale; 2) the observation station alternated between the boundary layer and the free troposphere, and the growth behaviors of new particles when new particle signals disappeared from the observations were unknown; and other sources of uncertainty. Thus, we further analyzed the D_{pgmax} in terms of the calculated particle GR, the observation duration of NPF events on site, and the underlying atmospheric processes.

Theoretically, the D_{pgmax} should be a function of the GR and the NPF duration. The GR is determined by real-time concentrations of condensation vapors, whereas the NPF duration is determined by the availability of condensation vapor over a certain long period, both of which are influenced by the concentration of oxidants (Zhang et al., 2012, Apsokardu and Johnston, 2018). In this study, a moderate correlation was observed between the D_{pgmax} and GR ($r = 0.5$, $p < 0.01$), suggesting that the GR alone does not determine the D_{pgmax}. When two outliers were removed, r increased to 0.68 (Fig. 7a). In addition, the GR showed a positive correlation with total oxidant ($O_x = NO_2 + O_3$), but with r as low as 0.38 ($p < 0.01$) (Fig. S5). Meanwhile, the D_{pgmax} and the duration of NPF events also showed good correlation ($r = 0.74$, $p < 0.01$) (Fig. 7e). Our results imply that both the real-time concentrations and the continuous supply of condensation vapor play dominant roles in growing new particles to the CCN size.

https://doi.org/10.5194/acp-2020-364
Preprint. Discussion started: 14 May 2020


Atmospheric Chemistry and Physics Discussions

To deepen the analysis, we considered three situations of the new particle growth. Type A (full marker in Fig. 7) represents that new particles continuously grow to the size of D_{pgmax} until the new particle signal drops to a negligible level. Type B (empty marker) represents the NPF events in which the growth of new particles is similar to that in Type A before the arrival of their D_{pgmax}. After the arrival of their D_{pgmax}, grown new particles in Type B can still be observed for one more hour, after which either the growth stops for over one hour or the particles start shrinking to a smaller size until the new particle signal disappears. Type C (half-full marker) represents the NPF events that are not subject to Type A or B. A multi-stage growth of new particles can be observed in Type C. A few examples of the three types are shown in Fig. S6. We also separated the observations in 2017 and 2018 (in red) from those in 2007–2015 (in blue).

For Type A, the averaged GR and D_{pgmax} in 2017–2018 were only 1.5 nm h^{-1} and 23 nm, respectively, which were significantly lower than 3.5 nm h^{-1} and 51 nm, respectively, observed in 2007–2015 ($p < 0.01$). The duration of NPF events showed no significant difference between 2017–2018 and 2007–2015. As reported in the literature, the lifetime of 50 nm particles in the boundary layer is approximately one day and is much longer in the free troposphere (Williams et al., 2002). It can be argued that the new particles in Type A of 2007–2015 may still have been able to grow to the CCN size even after the new particle signal disappeared from the observation. However, the lifetime of 20 nm particles in the boundary layer is only several hours (Williams et al., 2002). If the Type A NPF events in 2017–2018 occurred in the boundary layer, the new particles may not have been able to grow to the CCN size before being scavenged from the ambient air. If they occurred in the free troposphere, the longer lifetime may have allowed the new particles in some events to be able to grow to the CCN size. For example, the NPF event on March 21, 2018 ended with the increase in wind speed and change in wind direction, and the number concentration of new particles remained at a high level. The air mass back trajectories passed through the NCP at a high altitude (>1700 m a.g.l) at the beginning and end of the NPF event (Fig. S6a, b). In addition, the spikes of PNSDs during this NPF event indicated the vertical transport of atmospheric particles (Meng et al., 2015). We infer that this NPF event seemingly occurred in the free troposphere, and a large decrease in the entrainment from the free troposphere to the boundary layer may have led to the disappearance of the new particle signal. Recent aircraft and airship measurements in northern and eastern China suggested that NPF events sometimes occurred in the free troposphere and then mixed down to the boundary layer (Quan et al., 2017; Qi et al., 2019).

In the case of Type B, the GR and D_{pgmax} in 2017–2018 (the mean values of 3.2 nm h^{-1} and 29 nm, respectively) were also significantly lower than those in 2007–2015 (6.1 nm h^{-1} and 56 nm, respectively; $p < 0.01$). The number concentrations or the sizes of new particles decreased considerably at the end of Type B NPF events, and the transient time for the decrease suggested that the events occurred in the boundary layer. For example, the air mass back trajectories at the end of NPF on April 7, 2018 originated from low altitude, and the height varied greatly over time (Fig. S6c, d). Most of the Type B NPF events in 2017–2018 may have had less opportunity to contribute to the CCN population, if they indeed occurred in the boundary layer. However, aircraft measurements need to confirm at which altitude the NPF events occur.

https://doi.org/10.5194/acp-2020-364
Preprint. Discussion started: 14 May 2020


Atmospheric Chemistry and Physics Discussions

Type C was characterized by the largest GR, duration, and D_{pgmax}, with mean values of 7.7 nm h^{-1}, 26 h, and 98 nm, respectively. These particles underwent multiple growth processes. The air mass back trajectories at the end of the NPF event on September 30, 2014 were local and originated at a low altitude (Fig. S6e, f), implying that these new particles experienced sufficient growth within the boundary layer. There were 16 Type C NPF events during 2007–2015 and only two in 2017. The lack of Type C NPF events in 2017–2018 implies a significant decrease in the contribution of new particles to the CCN population.

The factors influencing the decreased D_{pgmax} and NPF-derived CCN population in 2017–2018 were further explored. The decrease in the mixing ratios of SO_2 and H_2SO_4 would reduce the contribution of H_2SO_4 to the growth of new particles. For example, the contribution of H_2SO_4 vapor to particle growth decreased from 36% in the spring of 2007 to 11% in the spring of 2018 (Table 2). However, this percentage is likely not high enough to explain the 50% decrease in the GR and D_{pgmax} in Types A and B. Meanwhile, the oxidant (O_x) concentrations were comparable between the two spring campaigns in 2007 and 2018 (Fig. 5c). Again, the changes in the VOC components and their condensation may be responsible for the significant decrease observed in the GR and D_{pgmax}. In 2018, the mixing ratio of TVOCs increased considerably. However, the mixing ratios of aromatic hydrocarbons showed a decreasing trend, i.e., from approximately 2.4 ppb in 2006 to 1.3 ppb in 2018, implying a decline in biomass and anthropogenic sources versus an increase in BVOC emissions. Furthermore, the reduction in SO_2 and sulfate may have reduced aerosol acidity, subsequently affecting the acid-enhanced uptake of semi-volatile organic species (Ding et al., 2011; Stangl et al., 2019). This hypothesis is supported by the lower level of organic carbon (OC) in $PM_{2.5}$ found in the spring of 2018 (5.5 ± 2.0 μg m^{-3}) than in the spring of 2007 (6.1 ± 3.0 μg m^{-3}), although TVOC emissions in 2018 were almost double those in 2007 (Table 2, Wang et al., 2011; Dong et al., 2020). Unfortunately, the chemical data of size-segregated molecular constituents are not available to confirm this finding, and therefore, more refined observations are urgently needed in the future.

5. Conclusions

With an order of magnitude reduction in SO_2 emissions, the NPF frequency observed at the summit of Mt. Tai remained relatively constant during 2007–2018. The calculated FR and NMINP were 0.8–1.2 cm^{-3} s^{-1} and 3.8–5.1 × 10^3 cm^{-3} in 2007–2014 and then unexpectedly increased by a factor of 2–3 in 2017–2018 to 2.0–3.0 cm^{-3} s^{-1} and 0.9–1.1 × 10^4 cm^{-3}, respectively. However, the large increase in the NPF intensity was accompanied by a smaller probability of the particles growing to the CCN size. The number concentrations of NPF-derived CCN with the three threshold sizes 50, 80, and 100 nm were estimated as 3703, 1556, and 861 cm^{-3} from 2007 to 2015, which then decreased to 1026, 456, and 176 cm^{-3}, respectively, in 2017 and 2018. On considering the three types of NPF events separately, it remains uncertain whether the new particles in Type A can grow to the CCN size after the disappearance of the new particle signals from observations. No conclusion can be drawn on this issue based on the current limited chemical observations. However, the new particles in Type B may have less opportunity to grow to the CCN size before they are scavenged from the ambient air. The lack of Type

https://doi.org/10.5194/acp-2020-364
Preprint. Discussion started: 14 May 2020


Atmospheric Chemistry and Physics Discussions

C NPF events in 2017–2018 indicates a large decrease in the probability of new particles growing to the CCN size with the reduction in ambient air pollutants. Moreover, shorter durations of the NPF events in 2017–2018 imply that the events occurred over a smaller spatial scale.

We hypothesize that the NPF intensity increased unexpectedly with the reduction in SO_2 concentrations, as the net production of NPF seems to be determined mainly by the availability of organic precursors for participating in nucleation and initial growth. The strong correlation between the FR and NMINP strongly supports this hypothesis, which needs to be further confirmed by direct observations of molecular organic vapors. A decrease in the percentage of new particles growing to the CCN size with increasing NPF intensity in 2017–2018 implies the complexity of the growth of new particles with reduced emissions of anthropogenic precursors. Overall, this study provides unique observational results regarding NPF at a regional mountain-top site in the NCP from reasonably large datasets. Based on the unique results, we analyzed the possible causes comprehensively, and proposed new challenges in determining the underlying mechanisms of the contributions of new particles to ambient particle number loading and CCN population with reduced anthropogenic emissions.

Data availability. The research data can be accessed upon contact with the corresponding author (Likun Xue, (xuelikun@sdu.edu.cn) and Xiaohong Yao (xhyao@ouc.edu.cn)).

Author contributions. LX designed the research. JC and JG conducted the field observations in 2007, 2014 and 2015. XW, HL, YZ, ZG, TC, LW, PZ, and YS carried out the field measurements in 2009, 2017 and 2018. YZ analyzed the data and wrote the paper. XY, TW and WW helped to interpretation of the results. XY and LX revised the original manuscript. All authors contributed toward improving the paper.

Competing interests. The authors declare that they have no conflict of interest.

Acknowledgements

This work was funded by the National Key Research and Development Program of China (2016YFC0200500), the National Natural Science Foundation of China (41922051, 41706122), Shandong Provincial Science Foundation for Distinguished Young Scholars (ZR2019JQ09), and the Jiangsu Collaborative Innovation Center for Climate Change. We appreciate the NOAA Air Resource Laboratory for providing the HYSPLIT model, and thank the staff of the Mt. Tai Meteorological Station for the help during the measurement campaigns.

https://doi.org/10.5194/acp-2020-364
Preprint. Discussion started: 14 May 2020


Atmospheric Chemistry and Physics Discussions

References

Apsokardu, M. J., and Johnston, M. V.: Nanoparticle growth by particle-phase chemistry, Atmos. Chem. Phys., 18, 1895–1907, https://doi.org/10.5194/acp-18-1895-2018, 2018.

Asmi, E., Kivekäs, N., Kerminen, V.-M., Komppula, M., Hyvärinen, A.-P., Hatakka, J., Viisanen, Y., and Lihavainen, H.: Secondary new particle formation in Northern Finland Pallas site between the years 2000 and 2010, Atmos. Chem. Phys., 11, 12959–12972, https://doi.org/10.5194/acp-11-12959-2011, 2011.

Charlson, R. J., Schwartz, S. E., Hales, J. M., Cess, R. D., Coakley, J. A., Hansen, J. E., and Hofmann, D. J.: Climate Forcing by Anthropogenic Aerosols. Science, 255, 423-430, 1992.

Chu, B., Kerminen, V. M., Bianchi, F., Yan, C., Petäjä, T., and Kulmala, M.: Atmospheric new particle formation in China. Atmos. Chem. Phys., 19, 115-138, https://doi.org/10.5194/acp-19-115-2019, 2019.

Dal Maso, M., Kulmala, M., Riipinen, I., Wagner, R., Hussein, T., Aalto, P. P., and Lehtinen, K. E. J.: Formation and growth of fresh atmospheric aerosols: Eight years of aerosol size distribution data from SMEAR II, Hyytiala, Finland, Boreal Environ. Res., 10, 323–336, 2005.

Ding, X., Wang, X., and Zheng, M.: The influence of temperature and aerosol acidity on biogenic secondary organic aerosol tracers: Observations at a rural site in the central Pearl River Delta region, South China, Atmos. Environ., 45, 1303-1311, https://doi.org/10.1016/j.atmosenv.2010.11.057, 2011.

Dong, S., Wang, X., Zhang J., Li, H., Li, W., Li, M., Gu, R., Jiang, Y., Shan, Y., Gao, X., Liu, H., Guo, Z., Xue, L., and Wang, W.: Light absorption properties, absorption contributions, and the influencing factors of atmospheric brown carbon on Mount Tai, Geochimica, 49, https://doi.org/10.19700/j.0379-1726.2020.01.011, 2020.

Dusek, U., Frank, G. P., Hildebrandt, L., Curtius, J., Schneider, J., Walter, S., Chand, D., Drewnick, F., Hings, S., Jung, D., Borrmann, S., and Andreae, M. O: Size matters more than chemistry for cloud-nucleating ability of aerosol particles, Science, 312, 1375–1378, https://doi.org/10.1126/science.1125261, 2006.

Ehn, M., Thornton, J. A., Kleist, E., Sipila, M., Junninen, H., Pullinen, I., Springer, M., Rubach, F., Tillmann, R., Lee, B., Lopez-Hilfiker, F., Andres, S., Acir, I.-H., Rissanen, M., Jokinen, T., Schobesberger, S., Kangasluoma, J., Kontkanen, J., Nieminen, T., Kurten, T., Nielsen, L. B., Jorgensen, S., Kjaergaard, H. G., Canagaratna, M., Dal Maso, M., Berndt, T., Petaja, T.,Wahner, A., Kerminen, V.-M., Kulmala, M.,Worsnop, D. R., Wildt, J., and Mentel, T. F.: A large source of lowvolatility secondary organic aerosol, Nature, 506, 476–479, https://doi.org/10.1038/nature13032, 2014.

Erupe, M. E., Benson, D. R., Li, J., Young, L. H., Verheggen, B., Al-Refai, M., Tahboub, O., Cunningham, V., Frimpong, F., Viggiano, A. A., and Lee, S. H.: Correlation of aerosol nucleation rate with sulfuricacid and ammonia in Kent, Ohio: An atmospheric observation, J. Geophys. Res. Atmos., 115, D23216, https://doi.org/10.1029/2010JD013942, 2010.

Fan, H., Zhao, C., and Yang, Y.: A comprehensive analysis of the spatio-temporal variation of urban air pollution in China during 2014–2018, Atmos. Environ., 220, 117066, https://doi.org/10.1016/j.atmosenv.2019.117066, 2020.

https://doi.org/10.5194/acp-2020-364
Preprint. Discussion started: 14 May 2020


Atmospheric Chemistry and Physics Discussions

Gao, J.: Study on aerosol number concentration, size distribution and the particle formation and growth process, Doctoral dissertation, Jinan, Shandong University, 2008.

Gao, J., Wang, T., Ding, A. J. and Liu, C. B.: Observational Study of Ozone and Carbon Monoxide at the Summit of Mount Tai (1534 m a.s.l.) in Central eastern China, Atoms. Envrion., 39, 4779–4791, 2005.

Gao, J., Wang, T., Zhou, X., Wu, W., and Wang, W.: Measurement of aerosol number size distributions in the Yangtze River delta in China: Formation and growth of particles under polluted conditions, Atmos. Environ., 43, 829-836, 2009.

Guo, H., Wang, D. W., Cheung, K., Ling, Z. H., Chan, C. K., and Yao, X. H.: Observation of aerosol size distribution and new particle formation at a mountain site in subtropical Hong Kong, Atmos. Chem. Phys., https://doi.org/10.5194/acp-12-9923-2012, 2012.

Hamed, A., Birmili, W., Joutsensaari, J., Mikkonen, S., Asmi, A., Wehner, B., Spindler, G., Jaatinen, A., Wiedensohler, A., Korhonen, H., Lehtinen, K. E. J., and Laaksonen, A.: Changes in the production rate of secondary aerosol particles in Central Europe in view of decreasing SO_2 emissions between 1996 and 2006, Atmos. Chem. Phys., 10, 1071–1091, https://doi.org/10.5194/acp-10-1071-2010, 2010.

Hirsikko, A., Bergman, T., Laakso, L., Dal Maso, M., Riipinen, I., Hõrrak, U., and Kulmala, M.: Identification and classification of the formation of intermediate ions measured in boreal forest, Atmos. Chem. Phys., 7, 201–210, https://doi.org/10.5194/acp-7-201-2007, 2007.

Kalivitis, N., Kerminen, V.-M., Kouvarakis, G., Stavroulas, I., Tzitzikalaki, E., Kalkavouras, P., Daskalakis, N., Myriokefalitakis, S., Bougiatioti, A., Manninen, H. E., Roldin, P., Petäjä, T., Boy, M., Kulmala, M., Kanakidou, M., and Mihalopoulos, N.: Formation and growth of atmospheric nanoparticles in the eastern Mediterranean: results from long-term measurements and process simulations, Atmos. Chem. Phys., 19, 2671–2686, https://doi.org/10.5194/acp-19-2671-2019, 2019.

Kerminen, V. M., Chen, X., Vakkari, V., Petäjä, T., Kulmala, M., and Bianchi, F.: Atmospheric new particle formation and growth: review of field observations, Environ. Res. Lett., 13, 103003, https://doi.org/10.1088/1748-9326/Aadf3c, 2018.

Kerminen, V.-M., Paramonov, M., Anttila, T., Riipinen, I., Fountoukis, C., Korhonen, H., Asmi, E., Laakso, L., Lihavainen, H., Swietlicki, E., Svenningsson, B., Asmi, A., Pandis, S. N., Kulmala, M., and Petäjä, T.: Cloud condensation nuclei production associated with atmospheric nucleation: a synthesis based on existing literature and new results, Atmos. Chem. Phys., 12, 12037–12059, https://doi.org/10.5194/acp-12-12037-2012, 2012.

Krotkov, N. A., McLinden, C. A., Li, C., Lamsal, L. N., Celarier, E. A., Marchenko, S. V., Swartz, W. H., Bucsela, E. J., Joiner, J., Duncan, B. N., Boersma, K. F., Veefkind, J. P., Levelt, P. F., Fioletov, V. E., Dickerson, R. R., He, H., Lu, Z., and Streets, D. G.: Aura OMI observations of regional SO_2 and NO_2 pollution changes from 2005 to 2015, Atmos. Chem. Phys., 16, 4605–4629, https://doi.org/10.5194/acp-16-4605-2016, 2016.

https://doi.org/10.5194/acp-2020-364
Preprint. Discussion started: 14 May 2020


Atmospheric Chemistry and Physics Discussions

Kulmala, M. and Kerminen, V. M.: On the formation and growth of atmospheric nanoparticles, Atmos. Res., 90, 132–150, https://doi.org/10.1016/j.atmosres.2008.01.005, 2008.

Kulmala, M., Dal Maso, M., Mäkelä, M., Pirjola, L., Väkevä, M., Aalto, P., Miikkulainen, P., and Hämeri, K.: On the formation, growth and composition of nucleation mode particles, Tellus B, 53, 479–490, https://doi.org/10.1034/j.1600-0889.2001.d01-33.x, 2001.

Kulmala, M., Petäjä, T., Nieminen, T., Sipilä, M., Manninen, H. E., Lehtipalo, K., Dao Maso, M., Aalto, P. P., Junninen, H., Paasonen, P., Riipinen, I., Lehtinen, K. E. J., Laaksonen, A., and Kerminen, V-M.: Measurement of the nucleation of atmospheric aerosol particles, Nat. Protoc., 7, 1651–1667, https://doi.org/10.1038/nprot.2012.091, 2012.

Kulmala, M., Vehkamäki, H., Petäjä, T., Dal Maso, M., Lauri, A., Kerminen, V.-M., Birmili, W., and McMurry, P. H.: Formation and growth rates of ultrafine atmospheric particles: a review of observations, J. Aerosol Sci., 35, 143–176, https://doi.org/10.1016/j.jaerosci.2003.10.003, 2004.

Lee, S., Gordon, H., Yu, H., Lehtipalo, K., Haley, R., Li, Y., and Zhang, R.: New particle formation in the atmosphere: From molecular clusters to global climate, J. Geophys. Res. Atmos., 124, 7098-7146, https://doi.org/10.1029/2018JD029356, 2019.

Li, K., Zhu, Y., Gao, H., and Yao, X.: A comparative study of cloud condensation nuclei measured between non-heating and heating periods at a suburb site of Qingdao in the North China, Atmos. Environ., 112, 40-53, https://doi.org/10.1016/j.atmosenv.2015.04.024, 2015.

Li, W. J., Zhang, D. Z., Shao, L. Y., Zhou, S. Z., and Wang, W. X.: Individual particle analysis of aerosols collected under haze and non-haze conditions at a high-elevation mountain site in the North China plain, Atmos. Chem. Phys., 11, 11733-11744, http://dx.doi.org/ 10.5194/acp-11-11733-2011, 2011.

Li, X., Zhao, B., Zhou, W., Shi, H., Yin, R., Cai, R., Yang, D., Dällenbach, K., Deng, C., Fu, Y., Qiao, X., Wang, L., Liu, Y., Yan, C., Kulmala, M., Zheng, J., Hao, J., Wang, S., and Jiang, J.: Responses of gaseous sulfuric acid and particulate sulfate to reduced SO2 concentration: A perspective from long-term measurements in Beijing, Sci. Total Environ., 137700, https://doi.org/10.1016/j.scitotenv.2020.137700, 2020.

Lihavainen, H., Kerminen, V.-M., Komppula, M., Hatakka, J., Aaltonen, V., Kulmala, M., and Viisanen, Y.: Production of "potential" cloud condensation nuclei associated with atmospheric newparticle formation in northern Finland, J. Geophys. Res.-Atmos., 108, 4782, doi:10.1029/2003JD003887, 2003.

Lv, G., Sui, X., Chen, J., Jayaratne, R., and Mellouki, A.: Investigation of new particle formation at the summit of Mt. Tai, China, Atmos. Chem. Phys., 18, 2243–2258, https://doi.org/10.5194/acp-18-2243-2018, 2018.

Ma, L., Zhu, Y., Zheng, M., Sun, Y., Huang, L., Liu, X., Gao, Y., Shen, Y., Gao, H., and Yao, X.: Investigating three patterns of new particles growing to cloud condensation nuclei size in Beijing's urban atmosphere, Atmos. Chem. Phys. Diss., 2020.

https://doi.org/10.5194/acp-2020-364
Preprint. Discussion started: 14 May 2020

Ma, M., Gao, Y., Wang, Y., Zhang, S., Leung, L. R., Liu, C., Wang, S., Zhao, B., Chang, X., Su, H., Zhang, T., Sheng, L., Yao, X., and Gao, H.: Substantial ozone enhancement over the North China Plain from increased biogenic emissions due to heat waves and land cover in summer 2017, Atmos. Chem. Phys., 19, 12195–12207, https://doi.org/10.5194/acp-19-12195-2019, 2019.

Ma, N., Zhao, C., Tao, J., Wu, Z., Kecorius, S., Wang, Z., Größ, J., Liu, H., Bian, Y., Kuang, Y., Teich, M., Spindler, G., Müller, K., van Pinxteren, D., Herrmann, H., Hu, M., and Wiedensohler, A.: Variation of CCN activity during new particle formation events in the North China Plain, Atmos. Chem. Phys., 16, 8593–8607, https://doi.org/10.5194/acp-16-8593-2016, 2016.

Man, H., Zhu, Y., Ji, F., Yao, X., Lau, N. T., Li, Y. J., Lee, B. P., and Chan, C. K.: Comparison of daytime and nighttime new particle growth at the HKUST Supersite in Hong Kong, Environ. Sci. Technol., 49, 7170–7178, https://doi.org/10.1021/acs.est.5b02143, 2015.

Mao, T., Wang, Y., Xu, H., Jiang, J., Wu, F., and Xu, X.: A study of the atmospheric VOCs of Mount Tai in June 2006, Atoms. Envrion., 43, 2503-2508, https://doi.org/10.1016/j.atmosenv.2009.02.013, 2009.

McMurry, P. H., Fink, M., Sakurai, H., Stolzenburg, M. R., Mauldin, III R. L., Smith, J., Eisele, F., Moore, K., Sjostedt, S., Tanner, D., Huey, L. G., Nowak, J. B., Edgerton, E., and Voisin D.: A criterion for new particle formation in the sulfur-rich Atlanta atmosphere, J. Geophys. Res. Atmos., 110, D22S02. https://doi.org/10.1029/2005JD005901, 2005.

Meng, H., Zhu, Y. J., Evans, G., and Yao, X. H.: An approach to investigate new particle formation in the vertical direction on the basis of high time-resolution measurements at ground level and sea level, Atmos. Environ., 102, 366-375, https://doi.org/10.1016/j.atmosenv.2014.12.016, 2015.

Merikanto, J., Spracklen, D. V., Mann, G. W., Pickering, S. J., and Carslaw, K. S.: Impact of nucleation on global CCN, Atmos. Chem. Phys., 9, 8601–8616, https://doi.org/10.5194/acp-9-8601-2009, 2009.

Mikkonen, S., Romakkaniemi, S., Smith, J. N., Korhonen, H., Petäjä, T., Plass-Duelmer, C., Boy, M., McMurry, P. H., Lehtinen, K. E. J., Joutsensaari, J., Hamed, A., Mauldin III, R. L., Birmili, W., Spindler, G., Arnold, F., Kulmala, M., and Laaksonen, A.: A statistical proxy for sulphuric acid concentration, Atmos. Chem. Phys., 11, 11319-11334, https://doi.org/10.5194/acp-11-11319-2011, 2011.

Nie, W., Ding, A., Wang, T., Kerminen, V., George, C., Xue, L., Wang, W., Zhang, Q., Petaja, T., Qi, X., Gao, X., Wang, X., Yang, X., Fu, C., and Kulmala, M.: Polluted dust promotes new particle formation and growth, Sci. Rep., 4, 6634. https://doi.org/10.1038/srep06634, 2014

Nieminen, T., Asmi, A., Dal Maso, M., Aalto, P. P., Keronen, P., Petäjä, T., Kulmala, M., and Kerminen, V-M.: Trends in atmospheric new-particle formation: 16 years of observations in a boreal-forest environment, Boreal Environ. Res., 19 191-214, 2014.

https://doi.org/10.5194/acp-2020-364
Preprint. Discussion started: 14 May 2020


Atmospheric Chemistry and Physics Discussions

Nieminen, T., Manninen, H. E., Sihto, S. L., Yli-Juuti, T., Mauldin, III R. L., Petäjä, T., Riipinen, I., Kerminen, V.-M., and Kulmala, M.: Connection of sulfuric acid to atmospheric nucleation in boreal forest, Environ. Sci. Technol., 43, 4715–4721. https://doi.org/10.1021/es803152j, 2009.

Paasonen, P., Nieminen, T., Asmi, E., Manninen, H. E., Petäjä, T., Plass-Dülmer, C., Flentje, H., Birmili, W., Wiedensohler, A., Hõrrak, U., Metzger, A., Hamed, A., Laaksonen, A., Facchini, M. C., Kerminen, V.-M., and Kulmala, M.: On the roles of sulphuric acid and low-volatility organic vapours in the initial steps of atmospheric new particle formation, Atmos. Chem. Phys., 10, 11223–11242, https://doi.org/10.5194/acp-10-11223-2010, 2010.

Petters, M. D., and Kreidenweis, S. M.: A single parameter representation of hygroscopic growth and cloud condensation nucleus activity, Atmos. Chem. Phys., 7, 1961–1971, https://doi.org/10.5194/acp-7-1961-2007, 2007.

Qi, X., Ding, A., Nie, W., Chi, X., Huang, X., Xu, Z., Wang, T., Wang, Z., Wang, J., Sun, P., Zhang, Q., Huo, J., Wang, D., Bian, Q., Zhou, L., Zhang, Q., Ning, Z., Fei, D., Xiu, G., and Fu, Q.: Direct measurement of new particle formation based on tethered airship around the top of the planetary boundary layer in eastern China, Atmos. Environ., 209, 92-101. https://doi.org/10.1016/j.atmosenv.2019.04.024, 2019.

Quan, J., Liu, Y., Liu, Q., Jia, X., Li, X., Gao, Y., Ding, D., and Wang, Z.: Anthropogenic pollution elevates the peak height of new particle formation from planetary boundary layer to lower free troposphere, Geophys. Res. Lett., 44, 7537-7543, https://doi.org/10.1002/2017GL074553, 2017.

Riipinen, I., Yli-Juuti, T., Pierce, J. R., Petäjä, T., Worsnop, D. R., Kulmala, M., and Donahue, N. M.: The contribution of organics to atmospheric nanoparticle growth, Nat. Geosci., 5, 453–458, https://doi.org/10.1038/ngeo1499, 2012.

Rose, C., Sellegri, K., Moreno, I., Velarde, F., Ramonet, M., Weinhold, K., Krejci, R., Andrade, M., Wiedensohler, A., Ginot, P., and Laj, P.: CCN production by new particle formation in the free troposphere, Atmos. Chem. Phys., 17, 1529-1541, https://doi.org/10.5194/acp-17-1529-2017, 2017.

Saha, P. K., Robinson, E. S., Shah, R. U., Zimmerman, N., Apte, J. S., Robinson, A. L., and Presto, A.: Reduced ultrafine particle concentration in urban air: changes in nucleation and anthropogenic emissions, Environ. Sci. Technol., 52, 6798–806, https://doi.org/10.1021/acs.est.8b00910, 2018.

Seinfeld, J.H. and Pandis, S.N.: Atmospheric chemistry and physics: From air pollution to climate change, John Wiley & Sons, New York, 2012.

Sellegri, K., Rose, C., Marinoni, A., Lupi, A., Wiedensohler, A., Andrade, M., Bonasoni, P., and Laj, P.: New Particle Formation: A Review of Ground-Based Observations at Mountain Research Stations, Atmosphere, 10, 493, https://doi.org/10.3390/atmos10090493, 2019.

Shen, L., Wang, H., Yin, Y., Chen, J., and Chen, K.: Observation of atmospheric new particle growth events at the summit of mountain Tai (1534 m) in Central East China, Atmos. Environ., 201, 148-157, https://doi.org/10.1016/j.atmosenv.2018.12.051, 2019.

555 Shen, X., Sun, J., Zhang, X., Kivekäs, N., Zhang, Y., Wang, T., Zhang, X., Yang, Y., Wang, D., Zhao, Y., and Qin, D.: Particle climatology in Central East China retrieved from measurements in planetary boundary layer and in free troposphere at a 1500-m-High mountaintop site, Aerosol Air Qual. Res, 16, 689-701, 2016a.

Shen, X. J., Sun, J. Y., Zhang, X. Y., Zhang, Y. M., Zhang, L., and Fan, R. X.: Key features of new particle formation events at background sites in China and their influence on cloud condensation nuclei, Fron. Environ. Sci. Eng., 10, 5,
560 https://doi.org/10.1007/s11783-016-0833-2, 2016b.

Sihto, S.-L., Kulmala, M., Kerminen, V.-M., Dal Maso, M., Petäjä, T., Riipinen, I., Korhonen, H., Arnold, F., Janson, R., Boy, M., Laaksonen, A., and Lehtinen, K. E. J.: Atmospheric sulphuric acid and aerosol formation: implications from atmospheric measurements for nucleation and early growth mechanisms, Atmos. Chem. Phys., 6, 4079–4091, https://doi.org/10.5194/acp-6-4079-2006, 2006.

565 Stangl, C. M., Krasnomowitz, J. M., Apsokardu, M. J., Tiszenkel, L., Ouyang, Q., Lee, S., and Johnston, M. V.: Sulfur dioxide modifies aerosol particle formation and growth by ozonolysis of monoterpenes and isoprene, J. Geophys. Res. Atmos., 124(8), 4800-4811. https://doi.org/10.1029/2018JD030064, 2019.

Stavrakou, T., Müller, J.-F., Bauwens, M., De Smedt, I., Van Roozendael, M., Guenther, A., Wild, M., and Xia, X.: Isoprene emissions over Asia 1979–2012: impact of climate and land-use changes, Atmos. Chem. Phys., 14, 4587–4605,
570 https://doi.org/10.5194/acp-14-4587-2014, 2014.

Sun, L., Xue, L., Wang, T., Gao, J., Ding, A., Cooper, O. R., Lin, M., Xu, P., Wang, Z., Wang, X., Wen, L., Zhu, Y., Chen, T., Yang, L., Wang, Y., Chen, J., and Wang, W., Significant increase of summertime ozone at Mount Tai in Central Eastern China, Atmos. Chem. Phys., 16, 10637–10650, https://doi.org/10.5194/acp-16-10637-2016, 2016.

Tröstl, J., Chuang, W. K., Gordon, H., Heinritzi, M., Yan, C., Molteni, U., Ahlm, L., Frege, C., Bianchi, F., Wagner, R.,
575 Simon, M., Lehtipalo, K., Williamson, C., Craven, J. S., Duplissy, J., Adamov, A., Almeida, J., Bernhammer, A.-K., Breitenlechner, M., Brilke, S., Dias, A., Ehrhart, S., Flagan, R. C., Franchin, A., Fuchs, C., Guida, R., Gysel, M., Hansel, A., Hoyle, C. R., Jokinen, T., Junninen, H., Kangasluoma, J., Keskinen, H., Kim, J., Krapf, M., Kuerten, A., Laaksonen, A., Lawler, M., Leiminger, M., Mathot, S., Moehler, O., Nieminen, T., Onnela, A., Petaejae, T., Piel, F. M., Miettinen, P., Rissanen, M. P., Rondo, L., Sarnela, N., Schobesberger, S., Sengupta, K., Sipila, M., Smith, J. N., Steiner, G., Tome, A.,
580 Virtanen, A., Wagner, A. C., Weingartner, E., Wimmer, D., Winkler, P. M., Ye, P., Carslaw, K. S., Curtius, J., Dommen, J., Kirkby, J., Kulmala, M., Riipinen, I., Worsnop, D. R., Donahue, N. M., and Baltensperger, U.: The role of low-volatility organic compounds in initial particle growth in the atmosphere, Nature, 533, 527–531, https://doi.org/10.1038/nature18271, 2016.

Wang, Y., Hopke, P. K., Chalupa, D. C., and Utell, M. J.: Long-term study of urban ultrafine particles and other pollutants,
585 Atmos. Environ., 45, 7672-7680, https://doi.org/10.1016/j.atmosenv.2010.08.022, 2011.

https://doi.org/10.5194/acp-2020-364
Preprint. Discussion started: 14 May 2020

Wang, Z., Birmili, W., Hamed, A., Wehner, B., Spindler, G., Pei, X. ,Wu, Z., Cheng, Y., Su, H., and Wiedensohler, A.: Contributions of volatile and nonvolatile compounds (at 300 °C) to condensational growth of atmospheric nanoparticles: an assessment based on 8.5 years of observations at the central Europe background site Melpitz, J. Geophys. Res. Atmos., 122, 485–97, https://doi.org/10.1002/2016JD025581, 2017.

Wang, Z., Wang, T., Gao, R., Xue, L., Guo, J., Zhou, Y., Nie, W., Wang, X., Xu, P., Gao, J., Zhou, X., Wang, W., and Zhang, Q.: Source and variation of carbonaceous aerosols at Mount Tai, North China: Results from a semi-continuous instrument, Atoms. Envrion., 45, 1655-1667, https://doi.org/10.1016/j.atmosenv.2011.01.006, 2011.

Wen, L., Xue, L., Wang, X., Xu, C., Chen, T., Yang, L., Wang, T., Zhang, Q., and Wang, W.: Summertime fine particulate nitrate pollution in the North China Plain: increasing trends, formation mechanisms and implications for control policy, Atmos. Chem. Phys., 18, 11261–11275, https://doi.org/10.5194/acp-18-11261-2018, 2018.

Whitby, K. T.: The physical characteristics of sulfur aerosols, Atoms. Envrion., 12, 135-159, 1978.

Williams, J., de Reus, M., Krejci, R., Fischer, H., and Ström, J.: Application of the variability-size relationship to atmospheric aerosol studies: estimating aerosol lifetimes and ages, Atmos. Chem. Phys., 2, 133–145, https://doi.org/10.5194/acp-2-133-2002, 2002.

Wu, Z. J., Hu, M., Liu, S., Wehner, B., Bauer, S., Ssling, A. M., Wiedensohler, A., Petaja, T., Dal Maso, M., and Kulmala, M.: New particle formation in Beijing, China: Statistical analysis of a 1-year data set, J. Geophys. Res.-Atmos., 112, D09209, https://doi.org/10.1029/2006jd007406, 2007.

Xie., H., Feng, L., Hu, Q., Zhu, Y., Gao, H., Gao, Y., and Yao, X.: Concentration and size distribution of water-extracted dimethylaminium and trimethylaminium in atmospheric particles during nine campaigns - Implications for sources, phase states and formation pathways, Sci. Total Environ., 130–141, https://doi.org/10.1016/j.scitotenv.2018.02.303, 2018.

Yao, L., Garmash, O., Bianchi, F., Zheng, J., Yan, C., Kontkanen, J., Junninen, H., Mazon, S.B, Ehn, M., Paasonen, P., Sipilä, M., Wang, M., Wang, X., Xiao, S., Chen, H., Lu, Y., Zhang, B., Wang, D., Fu, Q., Geng, F., Li, L., Wang, H., Qiao, L., Yang, X., Chen, J., Kerminen, V. M., Petäjä, T., Worsnop, D. R., Kulmala, M., and Wang. L.: Atmospheric new particle formation from sulfuric acid and amines in a Chinese megacity, Science, 361, 278-281, https://doi.org/10.1126/science.aao4839, 2018.

Zhang, R., Khalizov, A., Wang, L., Hu, M., and Xu, W.: Nucleation and growth of nanoparticles in the atmosphere, Chem. Rev., 112, 1957–2011, https://doi.org/10.1021/cr2001756, 2012.

Zhou, Y., Wang, T., Gao, X., Xue, L., Wang, X., Wang, Z., Gao, J., Zhang Q., and Wang, W.: Continuous observations of water-soluble ions in $PM_{2.5}$ at Mount Tai (1534 m asl) in central-eastern China, J. Atmos. Chem., 64, 107-127, https://doi.org/10.1007/s10874-010-9172-z, 2009.

Zhu, Y., Li, K., Shen, Y., Gao, Y., Liu, X., Yu, Y., Gao, H., and Yao, X.: New particle formation in the marine atmosphere during seven cruise campaigns, Atmos. Chem. Phys., 19, 89–113, https://doi.org/10.5194/acp-19-89-2019, 2019.

https://doi.org/10.5194/acp-2020-364
Preprint. Discussion started: 14 May 2020


Atmospheric Chemistry and Physics Discussions

Zhu, Y., Sabaliauskas, K., Liu, X., Meng, H., Gao, H., Jeong, C. H., Evans, G. J., and Yao, X.: Comparative analysis of new particle formation events in less and severely polluted urban atmosphere, Atmos. Environ., 98, 655–664, https://doi.org/10.1016/j.atmosenv.2014.09.043, 2014.

Zhu, Y., Yan, C., Zhang, R., Wang, Z., Zheng, M., Gao, H., Gao, Y., and Yao, X.: Simultaneous measurements of new particle formation at 1 s time resolution at a street site and a rooftop site, Atmos. Chem. Phys., 17, 9469–9484, https://doi.org/10.5194/acp-17-9469-2017, 2017.

Zhu, Y., Yang, L., Kawamura, K., Chen, J., Ono, K., Wang, X., Xue, L., and Wang, W.: Contributions and source identification of biogenic and anthropogenic hydrocarbons to secondary organic aerosols at Mt. Tai in 2014, Environ. Pollut., 220, 863-872, https://doi.org/10.1016/j.envpol.2016.10.070, 2017.

https://doi.org/10.5194/acp-2020-364
Preprint. Discussion started: 14 May 2020

Atmospheric Chemistry and Physics Discussions

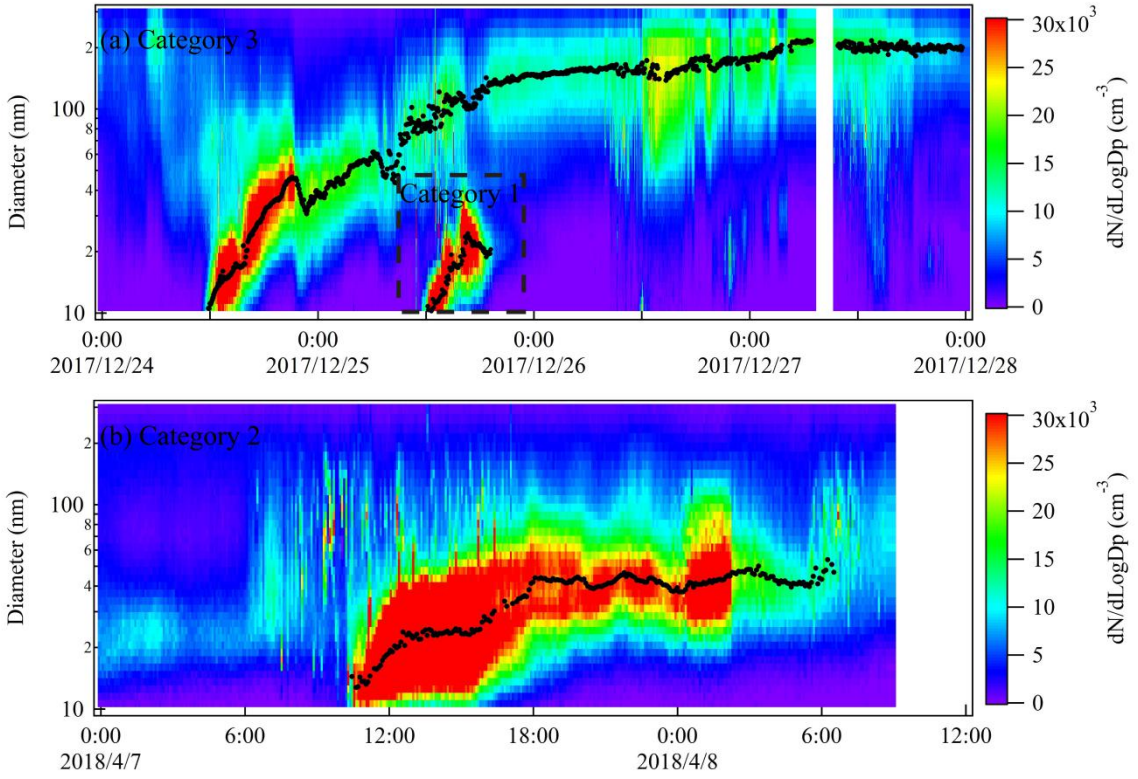

630 **Figure 1: Examples of NPF events in three categories. Black dots in the figures are the fitted D_{pg}. (a) Category 1 on December 25, 2017, in which D_{pgmax} was 24 nm (<50 nm), and Category 3 on December 24, 2017, in which D_{pgmax} grew to 217 nm (>80 nm); (b) Category 2 on April 7, 2018, in which D_{pgmax} grew to 55 nm (50–80 nm).**

https://doi.org/10.5194/acp-2020-364
Preprint. Discussion started: 14 May 2020

Atmospheric Chemistry and Physics Discussions

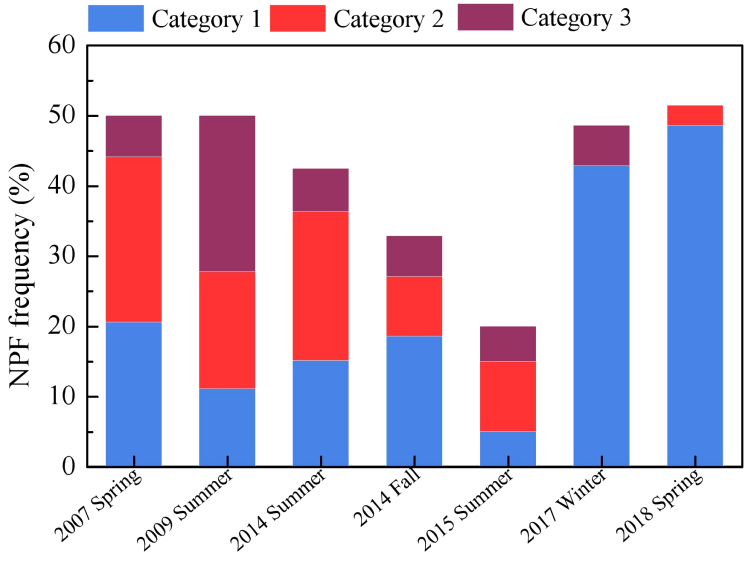

635

Figure 2: Occurrence frequencies of NPF events in different categories at Mt. Tai during the seven observation campaigns.

https://doi.org/10.5194/acp-2020-364
Preprint. Discussion started: 14 May 2020

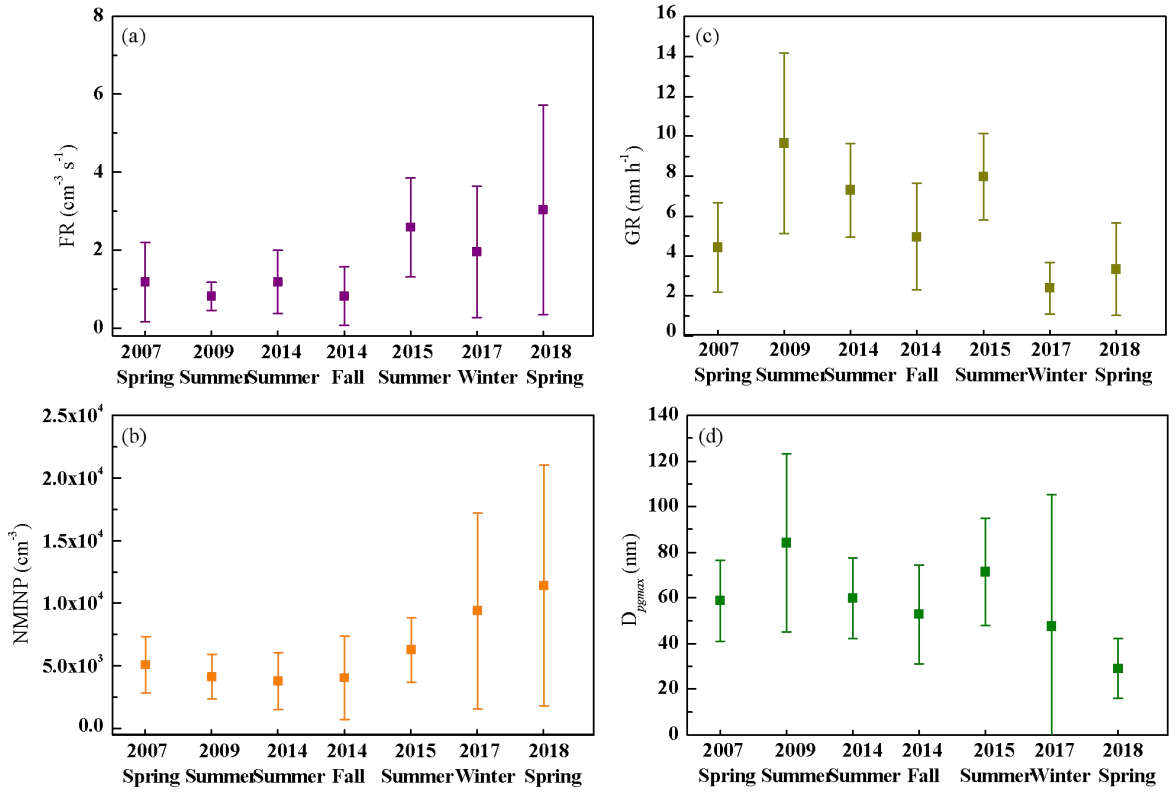

640 **Figure 3: Campaign average of new particle formation rate (FR, a), net maximum increase in the nucleation-mode particle number concentration (NMINP, b), new particle growth rate (GR, c), and maximum geometric median diameter of grown new particles (D_{pgmax}, d) during the seven observation campaigns. The error bars are the standard deviations.**

https://doi.org/10.5194/acp-2020-364
Preprint. Discussion started: 14 May 2020

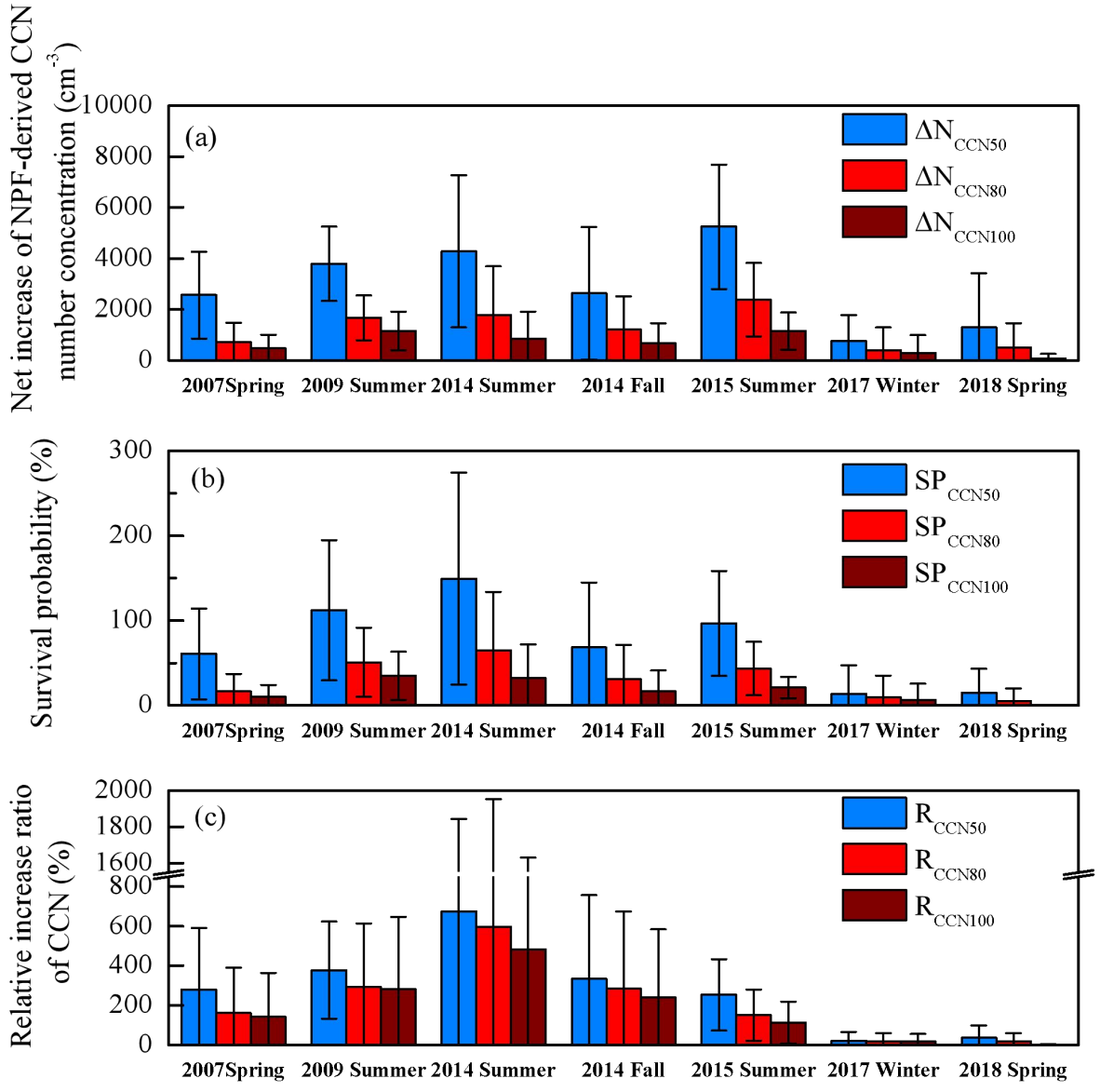

Figure 4: Campaign average of the net increase in NPF-derived CCN number concentration (ΔN_{CCN}, a), the survival probability of new particles to CCN sizes (SP_{CCN}, b), and the relative increase ratio of CCN population (R_{CCN}, c) during the seven observation campaigns. The error bars are the standard deviations.

https://doi.org/10.5194/acp-2020-364
Preprint. Discussion started: 14 May 2020

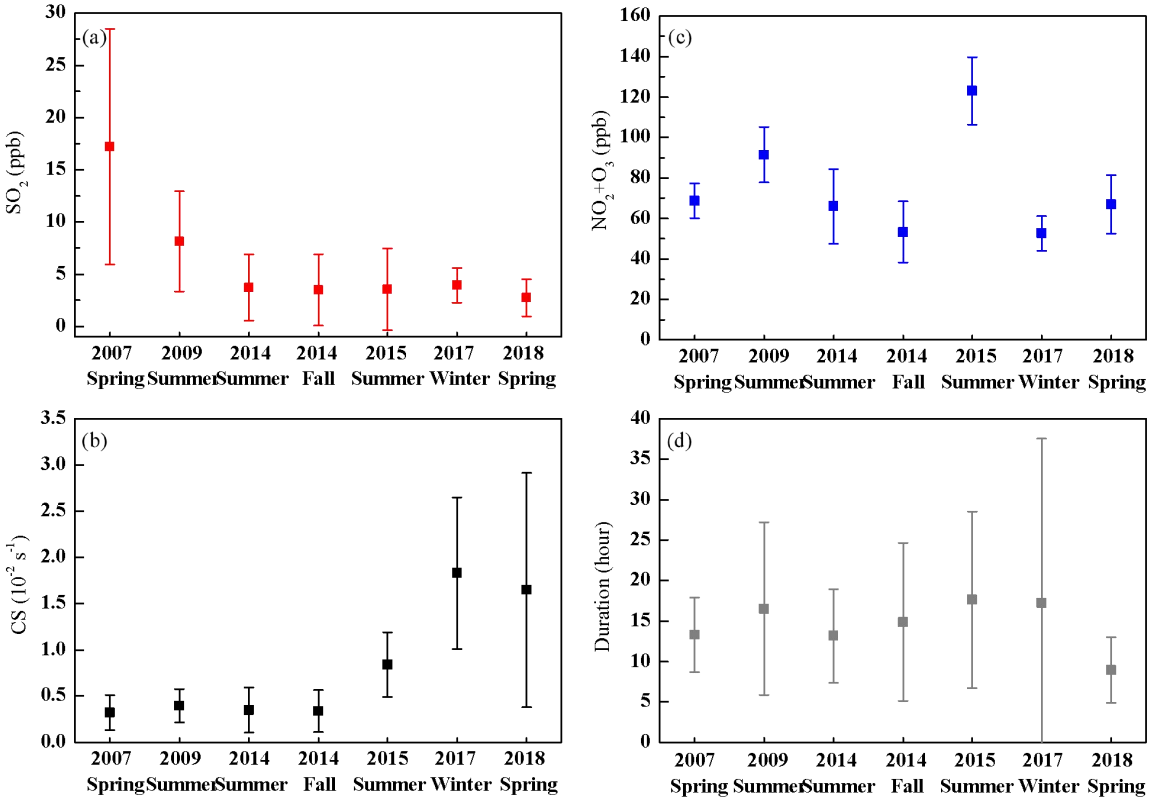

Figure 5: Campaign average of SO_2 mixing ratios (average during NPF periods, a), CS (one hour prior to NPF events, b), $NO_2 + O_3$ (average during new particle growth periods, c), and NPF event durations (d) during the seven observation campaigns. The error bars are the standard deviations.

https://doi.org/10.5194/acp-2020-364
Preprint. Discussion started: 14 May 2020

Atmospheric Chemistry and Physics Discussions

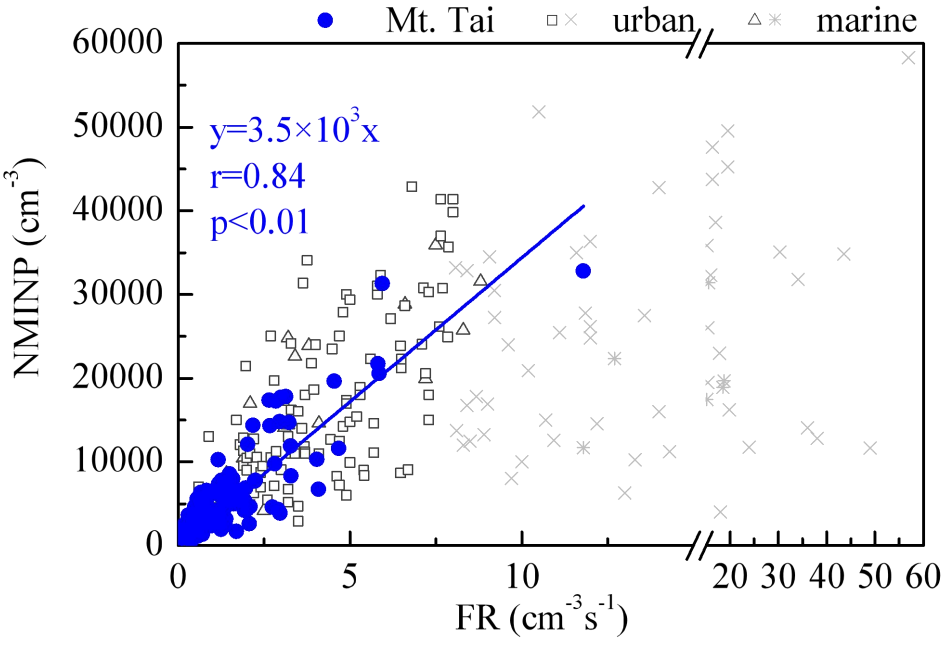

Figure 6: Relationship between the FR and NMINP in 106 cases of NPF events at Mt. Tai in this study and in urban and marine atmospheres in previous studies (Man et al., 2015; Zhu et al., 2017, 2019; Ma et al., 2020). Black markers can be fitted linearly in previous studies. Gray markers show poor correlations.

https://doi.org/10.5194/acp-2020-364
Preprint. Discussion started: 14 May 2020

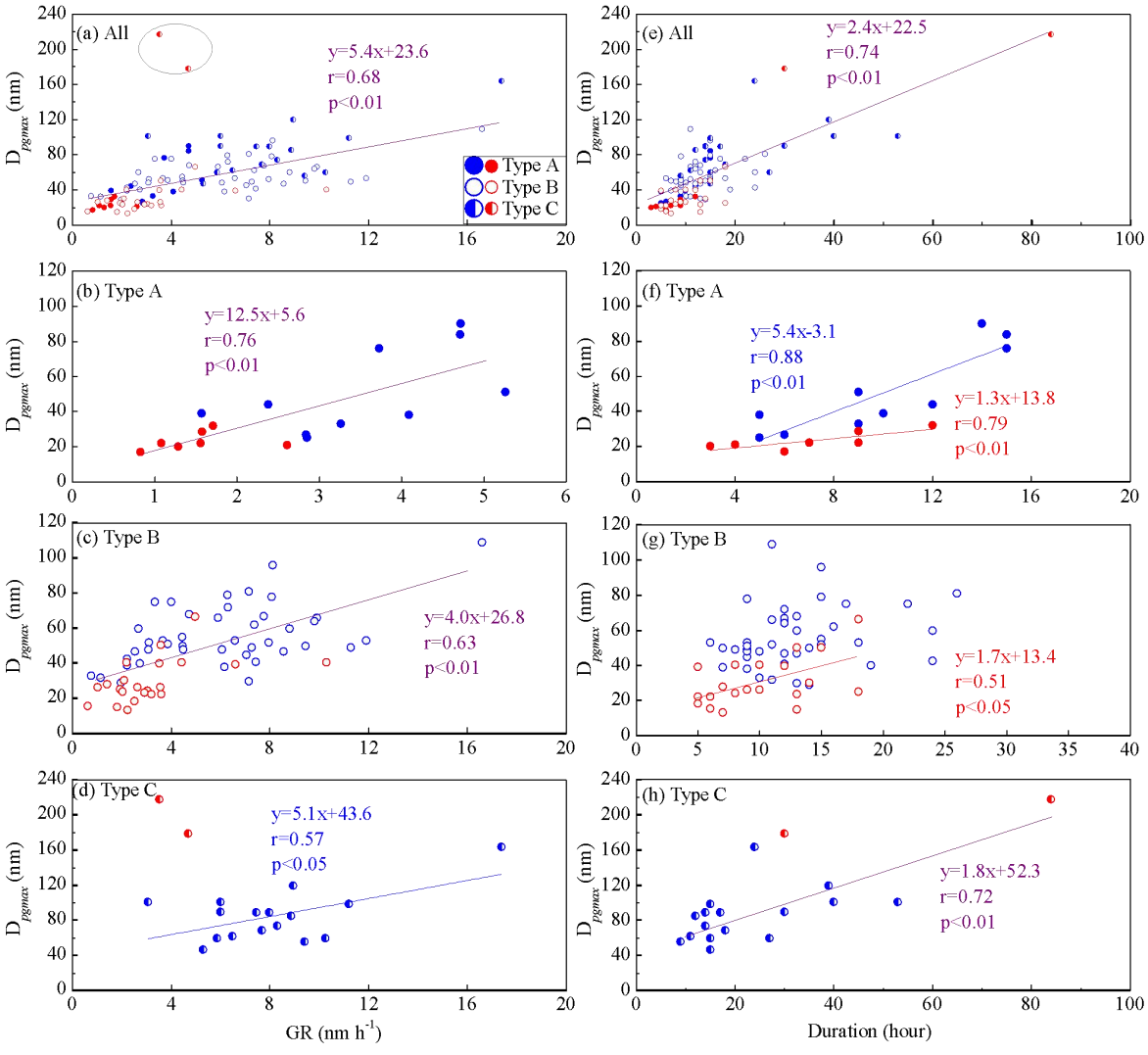

660 **Figure 7: Relationship between the GR and D_{pgmax} (a–d) and between the duration of NPF events and D_{pgmax} (e–h). Full marker represents Type A; empty marker represents Type B; and half full marker represents Type C. Red markers and equations represent 2017 and 2018, and blue markers and equations represent 2007–2015. Purple equation represents fitting of all data, and the circled markers represent the outliers when fitting the equation.**

665

https://doi.org/10.5194/acp-2020-364
Preprint. Discussion started: 14 May 2020


Atmospheric Chemistry and Physics Discussions

Table 1. Summary of the seven observation campaigns at Mt. Tai.

Campaign	Species	Instruments	Resolution
Spring 2007 3/22–4/24, 2007	PNSD in 10 nm–10 μm	WPS, MSP 1000XP	8 min
	SO_2, O_3, NO, and NO_2	Thermo 43C, 49C, 42C	1 min
	$PM_{2.5}$	TEOM 1400a	1 min
	Water-soluble ions in $PM_{2.5}$	URG-AIM 9000B	1 h
Summer 2009 6/12–6/29, 2009	PNSD in 10 nm–10 μm	WPS, MSP 1000XP	8 min
	SO_2, O_3, NO, and NO_2	Thermo 43C, 49C, 42C	1 min
Summer 2014 7/26–8/27, 2014	PNSD in 5 nm–10 μm	WPS, MSP 1000XP	5 min
	SO_2, O_3, NO, and NO_2	Thermo 43C, 49C,42i	1 min
	$PM_{2.5}$	Thermo 5030 SHARP	1 min
	Ions in $PM_{2.5}$, acid, and alkaline gases	MARGA, ADI20801	1 h
Fall 2014 9/21–11/30, 2014	PNSD in 5 nm–10 μm	WPS, MSP 1000XP	5 min
	SO_2, O_3	Thermo 43C, 49C	1 min
	NO, NO_2	API T200U, T500U	1 min
	$PM_{2.5}$	Thermo 5030 SHARP	1 min
	Ions in $PM_{2.5}$, acid, and alkaline gases	MARGA, ADI20801	1 h
Summer 2015 6/16–7/25, 2015	PNSD in 5 nm–10 μm	WPS, MSP 1000XP	5 min
	SO_2, O_3	Thermo 43C,49C	1 min
	NO, NO_2	API T200U, T500U	1 min
	$PM_{2.5}$	Thermo 5030 SHARP	1 min
	Ions in $PM_{2.5}$, acid, and alkaline gases	MARGA, ADI20801	1 h
Winter 2017 11/26–12/30, 2017	PNSD in 5 nm–10 μm	WPS, MSP 1000XP	5 min
	SO_2, O_3	Thermo 43C, API 400U	1 min
	NO, NO_2	API T200U, T500U	1 min
	$PM_{2.5}$	Thermo 5030 SHARP	1 min
	Ions in $PM_{2.5}$, acid, and alkaline gases	MARGA, ADI20801	1 h
Spring 2018 3/5–4/8, 2018	PNSD in 5 nm–10 μm	WPS, MSP 1000XP	5 min
	SO_2, O_3	Thermo 43C, API 400U	1 min
	NO, NO_2	API T200U, T500U	1 min
	$PM_{2.5}$	Thermo 5030 SHARP	1 min
	Ions in $PM_{2.5}$, acid, and alkaline gases	MARGA, ADI20801	1 h

https://doi.org/10.5194/acp-2020-364
Preprint. Discussion started: 14 May 2020

Atmospheric Chemistry and Physics Discussions

Table 2. Meteorological conditions and air pollutants during the formation and growth periods of new particles in the spring campaigns in 2007 and 2018.

Parameters	2007 spring		2018 spring	
	Formation	Growth	Formation	Growth
T (℃)	5.8 ± 3.2	7.1 ± 3.3	3.5 ± 5.8	5.3 ± 5.9
RH (%)	54 ± 22	52 ± 18	45 ± 17	46 ± 17
SO_2 (ppb)	16.7 ± 10.9	20.2 ± 13.0	2.6 ± 1.8	2.5 ± 1.5
NH_3 (ppb)	12.6 ± 18.0	11.2 ± 17.0	6.5 ± 9.5	6.6 ± 7.2
$NO_2 + O_3$ (ppb)	63.7 ± 8.4	70.1 ± 9.7	61.3 ± 14.0	63.8 ± 14.3
$PM_{2.5}$ (μg m^{-3})	56.5 ± 33.0	71.1 ± 49.0	30.3 ± 21.8	29.2 ± 20.4
SO_4^{2-} (μg m^{-3})	16.9 ± 11.2	18.5 ± 9.9	3.2 ± 2.4	3.6 ± 2.7
Calculated H_2SO_4 (10^7 molecules·cm^{-3})	8.8 ± 4.9	9.4 ± 4.5	2.2 ± 1.1	2.4 ± 1.0
$[H_2SO_4]_{avg}/C$ (%)	59 ± 23	36 ± 18	23 ± 10	11 ± 7
TVOC (ppb)	7.0 ± 5.7[a]		16.1 ± 6 .5	
OC (μg m^{-3})	6.1 ± 3.0[b]		5.5 ± 2.0[c]	
EC (μg m^{-3})	1.8 ± 1.6 [b]		1.3 ± 0.6 [c]	

[a](Mao et al., 2009)
[b](Wang et al., 2011)
[c](Dong et al., 2020)